

A Comparative Analysis of the Visual Comfort Performance between a PCM Glazing and a Conventional Selective Double Glazed Unit

*Original*

A Comparative Analysis of the Visual Comfort Performance between a PCM Glazing and a Conventional Selective Double Glazed Unit / Giovannini, Luigi; Goia, Francesco; Lo Verso, Valerio R. M.; Serra, Valentina. - In: SUSTAINABILITY. - ISSN 2071-1050. - ELETTRONICO. - 10:10(2018), pp. 1-20. [10.3390/su10103579]

*Availability:*

This version is available at: 11583/2715035 since: 2018-10-12T14:45:42Z

*Publisher:*

MDPI

*Published*

DOI:10.3390/su10103579

*Terms of use:*

This article is made available under terms and conditions as specified in the corresponding bibliographic description in the repository

*Publisher copyright*

(Article begins on next page)

## Article

# A Comparative Analysis of the Visual Comfort Performance between a PCM Glazing and a Conventional Selective Double Glazed Unit

Luigi Giovannini <sup>1,\*</sup>, Francesco Goia <sup>2</sup> , Valerio R. M. Lo Verso <sup>1</sup> and Valentina Serra <sup>1</sup>

<sup>1</sup> TEBE Research Group, Department of Energy, Politecnico di Torino, C.so Duca degli Abruzzi 24, 10129 Turin, Italy; valerio.loverso@polito.it (V.R.M.L.V.); valentina.serra@polito.it (V.S.)

<sup>2</sup> Department of Architecture and Technology, Faculty of Architecture and Design, Norwegian University of Science and Technology, Alfred Getz' vei 3, 7491 Trondheim, Norway; francesco.goia@ntnu.no

\* Correspondence: luigi.giovannini@polito.it; Tel.: +39-011-090-45-47

Received: 9 September 2018; Accepted: 2 October 2018; Published: 8 October 2018



**Abstract:** The performance of a Double Glazing Unit (DGU) with a Phase Change Material (PCM) layer embedded in the cavity was analyzed in terms of the visual comfort perceived by the occupants. The analysis was carried out through a set of simulations, performed by the Radiance engine managed through Honeybee. As an input for the simulations, the visible transmittance  $T_v$  of PCM in solid (diffusing) state was used, based on previous laboratory measurements. The simulations were run for several specific times of the year: The two solstices and the autumn equinox, for different hours during the day. Other variables investigated were the site (Östersund, 63.2° N; Turin, 45.2° N; Abu Dhabi, 24.4° N), the room orientation (south; west), and the sky conditions (clear sky with sun; overcast). For comparative purpose, the simulations were repeated for the same boundary conditions in a room equipped with a selective glazing, with a  $T_v$  of 0.5. For each case, the visual comfort perceived by the occupants has been analyzed in terms of Daylight Glare Probability (*DGP*) in two different points in the room and of “Spatial Useful Illuminance” (percent of work plane points where the illuminance lies in the range 100–3000 lx). The results showed that the glazed package with PCM in most cases admits more daylight into the room, resulting into an increased glare (*DGP* values), but also in lower Spatial Useful Illuminance values.

**Keywords:** visual comfort; glare; phase change material (PCM); daylight simulation; Daylight Glare Probability; Spatial Useful Illuminance; Radiance simulations

## 1. Introduction

### 1.1. Background

Over the last decade, the building envelope has received a special attention as a key factor to control and reduce energy use in buildings, focusing on the improvement of both its opaque and transparent components. As far as the transparent component is concerned, different solutions have been developed and tested, especially in the direction of making the building envelope acting as a “living” membrane [1], that is to say that the building envelope is conceived as an ‘active’ filter, able to dynamically change its performance in response to the outside boundary conditions. As a result, heat and mass flows are optimized dynamically in order to improve the comfort conditions perceived by the occupants (in the perspective of an Indoor Environmental Quality approach) as well as to reduce the energy the building requires to guarantee comfort [2].

In this context, different technologies and materials can be used to obtain an adaptive performance of the active envelope. The adaptive behavior can be pursued at the scale of different components, and/or with a different time scale: For instance, switchable layers can be used [3]; alternatively, an air flow can be implemented in a specifically devoted cavity [4,5]; or a phase change material (PCM) can be integrated into a Double Glazing Unit (DGU) [6]. The control capabilities of an adaptive façade simultaneously involve several phenomena: Thermal and solar fluxes, admitted daylighting, and air mass flows. A façade that aims at optimizing one aspect alone shows inevitably some influence on the performance of all the other aspects, with an inter-connected effect that is not always easy to predict. Furthermore, each technology presents a specific, different degree of “dynamicity” that is the capability of reacting to the external conditions. As a result, these façades are particularly difficult to be characterized and modelled into conventional energy/comfort models and simulation tools. A substantial lack of dedicated metrics and standard evaluation procedures is also to be highlighted when it comes to the need to quantify the performances of adaptive façades in an integrated way. All these aspects limit a more widespread use of these technologies. On the contrary, within the holistic approach to energy and indoor environmental performance of the façade components, requirements concerning energy, lighting, and acoustical behavior have to be contemporarily satisfied, even in such a multi-criteria setting.

### 1.2. Visual Comfort

Typically, adaptive façades have been studied focusing only on one aspect (energy performance, or thermal comfort performance, or visual comfort performance, and so forth) for the sake of simplicity. Even when the focus is limited to a particular topic, such as the visual comfort perceived in an indoor space, the performance criteria to be used are not defined in a unique way [7,8]. Following the current standards in this field [9], the visual comfort condition is analyzed in terms of: (i) quantity and distribution of light inside a space (typically the workplace), through the average illuminance and the illuminance uniformity; (ii) glare potentially perceived by the occupants, through glare indices that are based on the luminance distribution in the occupants’ field of view.

When the visual comfort needs to be assessed under daylighting conditions, specific daylight metrics are used to fully address the human perception of the luminous environment. These metrics need to account for both the temporal and spatial daylight variation, as the daylight environment across a space dynamically changes with time. Integrating such spatial and temporal variables into one metric is a quite complex challenge, which can become even more problematic for the case of a glazing component that exhibits dynamic optical properties.

As far as the glare risk is concerned, the position of the occupants in the space and the physiological-psychological aspects such as the subjective adaptation to the luminous environment play an even greater role. These aspects further increase the complexity of the problem, as well as of the development of predictive metrics. Presently, the most reliable glare metric to be used as reference for daylit spaces is the Daylight Glare Probability (DGP) [10]. This was validated for side-lit office spaces and connects the glare perception of the occupants to the luminance of daylight sources and to the vertical illuminance recorded at their eyes.

A number of studies have addressed the topic of visual comfort for users through the glare risk in the presence of adaptive transparent façades. Konstantzos et al. [11] studied the visual comfort concerned with dynamic fenestrations with shading systems, while Piccolo et al. [12] investigated the effect on comfort of switchable glass panes. An interesting study from Matusiak [13] was conducted on a static translucent façade (with a total visible transmittance of 0.29). This research showed that in the presence of a translucent façade, the occupants may also experience a high glare sensation. In the same study the hypothesis is also discussed that allowing a view to the outside of the building may reduce the sensation of discomfort, due to a psychological compensation [14,15], concluding that such hypothesis cannot be confirmed.

Studies on translucent glazing represent an interesting benchmark against which a technology based on the integration of a PCM into a DGU can be compared, especially when the PCM layer is in solid diffusing state. As far as PCMs are concerned, several studies are available in the literature on the thermal and the energy performance associated with their use, based on extensive numerical and experimental analyses, as well as comprehensive literature reviews [6,16,17]. On the contrary, the impact of PCM integrated in DGU on the visual comfort for the occupants has not been addressed so far, if not by a preliminary study by the same authors of this paper [18]. This is probably due to the fact that analyzing the optical behavior of PCMs is a quite complex matter, as the transmission properties change with the state. When in liquid state, the PCM transmission is specular, similarly to what happens for a typical clear glazing; when in solid state, the scattering phenomena inside the PCM prevail and the transmission mode is diffuse, similarly to what happens for a translucent transparent material. During the transition phase, the behavior is more complex as an intermediate between specular and diffusing, even though the diffusing mode is still predominant.

The integration of PCMs into a glazing system is meant to improve the thermal inertia of a transparent envelope component, and consequently its global energy performance in terms of better exploitation of the solar energy. Furthermore, considering that many PCMs are partially transparent materials, the adoption of such a system allows daylight to be admitted into an interior space. Over the last few years, several configurations with PCM layers integrated have been tested or simulated, including simple systems (e.g., a DGU where the cavity is filled with a PCM [19–23], up to more complex solutions, which use triple-glazed units [24,25] equipped with dynamic glass panes [26,27], prismatic glass panes [28–30] or additional insulation materials [31].

### 1.3. Aims of the Paper

Within this context, this paper originates from a preliminary study presented at the Sustainability in Energy and Buildings 2016 (SEB-16) conference [18], with the aim of complementing the state of the art on the performance of PCM glazing with a dedicated investigation on their impact on the luminous environment and on the visual comfort that may be experienced by the users. For this purpose, the *DGP* was adopted in this investigation to analyze the visual comfort provided by the glazing system. The Radiance based tool *Evalglare* was used for the purpose. Moreover, a new spatial metric was introduced by the Authors to complement the analysis, the "*Spatial Useful Illuminance*", which is defined as the percent of workplane points that have a horizontal illuminance within a certain "comfort range". As mentioned, the present paper expands the earlier study [18] by introducing a wider range of variables, such as the orientation (the target room is assumed with the DGU facing west, to complement the earlier study with the DGU facing south) and for an overcast sky, to complement the initial condition of a clear sky with sun.

For both the earlier and the present study, the focus is placed on the solid state case only. This choice was made for two reasons. Firstly, the liquid state is characterized by a specular behavior, which is a well-known phenomenon and is (relatively) easy to model; the impact of a PCM layer in liquid state on the luminous environment can be thus easily foreseen knowing the behavior of specular glazed systems. Secondly, the optical properties of the solid state are similar to that of the transition phase, and represent a more challenging condition, due to the scattering behavior (dominant diffuse transmission). The transition phase is the ideal condition of operation for the PCM layer, since an optimized PCM glazing should always be maintained in the transition phase in order to guarantee the best performance in terms of energy efficiency and thermal comfort.

Among all the possible glazing configurations explored by the research community within this concept, a very simple solution, which consists of a clear DGU with paraffin wax filling the cavity, was used in the present study. This choice was done to make the conclusions more general and relevant to the use of the PCM layer alone—i.e., if additional technologies/components (such as the presence of further insulation layers or of shading systems) are included, it can be more difficult to understand the effects are of each sub-component independently. The PCM configuration adopted in the study was

characterized experimentally in a test cell facility, where the thermophysical behavior and the energy performance were measured [20]. Furthermore, the implications on the thermal comfort conditions have been previously explored [19], as well as the full optical characterization performed [32,33], through a test-cell and laboratory analysis, respectively.

The study presented in this paper is based on simulations that were carried out using the lighting simulation tool *Radiance*. The visible transmittance values  $T_v$  of the DGU were measured earlier in laboratory [33] and then used as input data in the Radiance model. A set of simulations was carried out for some reference days during the course of a year, at various hours, leading to a new understanding of the visual comfort performance of these systems under different boundary conditions.

Furthermore, the methodology used to analyze the visual comfort in the sample space due to the PCM (both to run simulation and to post-process data and to visualize and communicate the results of the performance metrics) is also innovative. This was adopted for the case-study of this paper, but it is intended to have a more general application for the characterization of the visual comfort performance of adaptive transparent components in general.

## 2. Materials and Methods

### 2.1. Description of the Glazing Systems Used for the Simulations

The DGU integrating the PCM layer consists of a double pane extra-clear glass (each with a thickness of 4 mm) and a 15 mm thick air gap, completely filled with commercial grade paraffin wax [20].

As previously mentioned, the transmittance/reflectance properties of the PCM were characterized in laboratory for the material in the solid state, using an Ulbricht sphere with large diameter (75 cm) and a spectrophotometer [33]. The measures showed that in solid state the PCM is a translucent material with a nearly Lambertian behavior. The following measured visible transmittance, reflectance and absorptance were found:  $T_v = 0.55 \pm 0.02$ ;  $R_v = 0.33 \pm 0.02$  and  $A_v = 0.14 \pm 0.02$  [33].

For comparative purposes, a specular glass with the same visible transmittance as the DGU with PCM was also selected. A selective glass with a  $T_v$  of 0.5 was chosen for this purpose. This 'standard' glazing has been used as a baseline against which to compare the performance of the DGU with the PCM.

### 2.2. Description of the Case Study and of the Simulation Approach

A standard single office was defined as sample room for the study. The room had a width of 3.6 m, a depth of 5 m, and a height of 2.7 m (Figure 1). It was assumed to be daylight through a single window, positioned in one of the short walls, and with a surface that entirely covered the wall surface, thus resulting in a window-to-wall ratio of 1. The window was subdivided through mullions and frames into nine modules. The three modules in the middle section were 1.2 m in height while the three modules in the lower and upper sections of the window are 0.75 m in height each. This window layout was defined in accordance with one of the most common configurations used in many façades of office buildings. In the simulations, the DGU with PCM component and with the specular glazing were applied to the entire window (9 DGUs).

The comparison between the DGU with PCM and the DGU made of selective glass panes was carried out under different boundary conditions in terms of climate and orientation.

As far as the climate is concerned, the room was located in three different sites: Östersund, Sweden (latitude  $L = 63.2^\circ$  N, longitude  $l = 14.5^\circ$  E); Turin, Italy ( $L = 45.2^\circ$  N,  $l = 7.65^\circ$  E); Abu Dhabi, United Arab Emirates ( $L = 24.4^\circ$  N,  $l = 54.65^\circ$  E). The latitudes of the 3 sites differ of approximately  $20^\circ$  from one another, and this allowed the potential effect of latitude on the technology performance to be evaluated.

When it comes to the orientation, the sample office was oriented south and west for every site, alternatively. East and west orientations are quite similar from a lighting viewpoint, but, as the usual occupancy profile of a standard office sees the early morning hours as unoccupied, the afternoon hours (corresponding to a west orientation of the window) were selected for this study, as these may cause

more discomfort problems for the occupants. The north orientation was not investigated because the PCM glazed technology is only planned to be used in orientations that present relevant direct radiation—diffuse radiation is not sufficient to activate the PCM layer and thus to exploit the features of this technology in terms of control of solar gain [20].

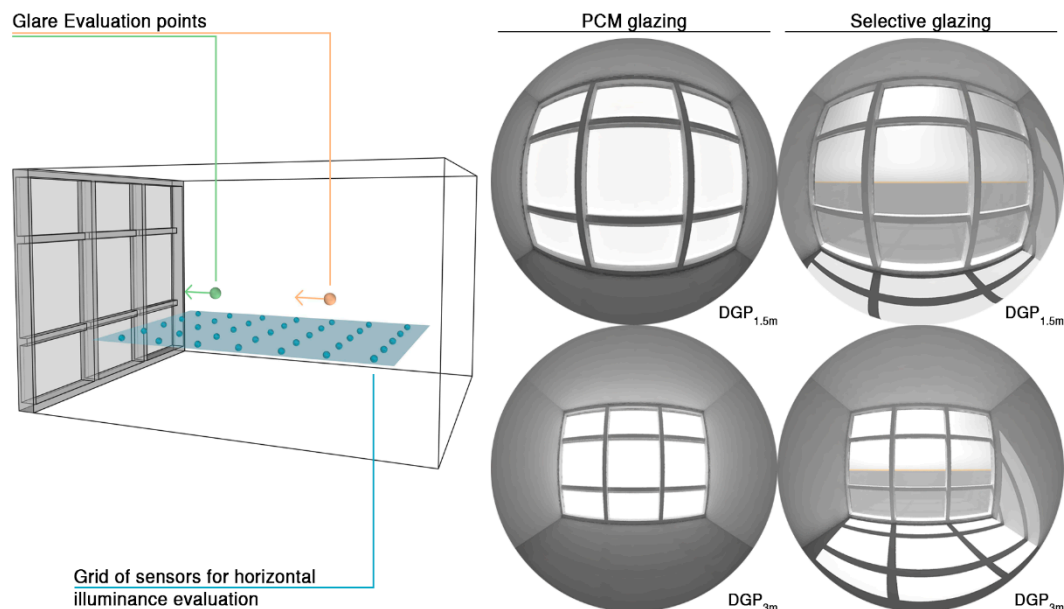


**Figure 1.** Model of the sample office room, where the sensor grid to calculate the illuminance values [blue] and the DGP [orange/green] are shown (left), and visualization of some images that were used to calculate  $DGP_{1.5m}$  and  $DGP_{3m}$  (right).

Three meaningful times of the year were chosen to run the simulations: The summer solstice (21 June), the autumn equinox (21 September), and the winter solstice (21 December). These three days are useful to describe the variation of sun positions during the course of a year, as they range from the minimum values of solar elevation and irradiance (winter), to the maximum values (summer), also including an intermediate situation (autumn equinox). For each of these days, the simulations were run for the following hours: 9:00, 12:00 (noon), 15:00, and 18:00. The solar angles for all the cases considered are shown in Table 1.

**Table 1.** Solar angles for the three sites for the time-steps considered in the study.  $\alpha$  = solar azimuth angle [ $^{\circ}$ ];  $\gamma$  = solar elevation angle [ $^{\circ}$ ]. Where  $\alpha$  and  $\gamma$  values are missing [–], the sun has already set.

		Östersund		Turin		Abu Dhabi	
		$\alpha$ [ $^{\circ}$ ]	$\gamma$ [ $^{\circ}$ ]	$\alpha$ [ $^{\circ}$ ]	$\gamma$ [ $^{\circ}$ ]	$\alpha$ [ $^{\circ}$ ]	$\gamma$ [ $^{\circ}$ ]
21 June	09:00	120.6	40.0	98.9	42.3	80.3	43.9
	12:00	178.7	50.3	161.2	67.3	99.5	84.6
	15:00	237.4	40.7	246.7	52.8	276.7	54.3
	18:00	280.3	21.2	281.9	21.7	289.5	14.4
21 September	09:00	132.7	19.8	119.7	27.1	109.1	37.4
	12:00	181.4	27.6	172.0	45.4	170.9	66.1
	15:00	229.7	18.8	229.6	33.6	245.7	43.5
	18:00	271.4	0.02	266.4	4.4	269.1	3.6
21 December	09:00	–	–	133.4	6.7	130.9	22.0
	12:00	180.0	3.4	173.3	21.1	174.1	41.9
	15:00	–	–	215.6	13.1	222.2	28.3
	18:00	–	–	–	–	–	–



The simulations were repeated under two different sky conditions, the CIE standard clear sky with sun and the CIE standard overcast sky. This approach was adopted to evaluate the performance of the technologies both in the presence and in the absence of direct solar radiation. In total, 288 different cases were obtained (and simulated) from the combination of all the above variables.

The validated lighting software Radiance was used to run the simulations and the following simulation parameters were adopted:  $-ab = 5$ ,  $-ad = 1024$ ,  $-as = 256$ ,  $-ar = 256$ ,  $-aa = 0.05$ . The simulation procedure was managed through three parametric tools integrated with the NURBS-based CAD environment Rhinoceros: Grasshopper, used to model the sample office; Ladybug and Honeybee (two add-on of Grasshopper), used to apply Radiance compatible materials to each surface of the model (Ladybug) and to run the simulations (Honeybee). Using Ladybug and Honeybee made it possible to run the simulations with the Radiance engine in a parametric way. A great number of analyses was therefore automatically run in sequence and the results processed afterwards according to specific, user-defined necessities.

In the Radiance model, *plastic* (Lambertian) materials were applied to all the opaque surfaces, with the following  $R_v$  values: 0.8 for the ceiling, 0.65 for the walls, 0.35 for the floor, 0.75 for the window frame, and 0.15 for the outside ground (albedo). A *trans* material (featuring a diffuse transmission) was instead used to model the PCM component. This *trans* material was specifically created for this application, using as input data the direct and diffuse transmittance/reflectance values that were experimentally measured in laboratory [33]. Table 2 contains the input values that were used: Values equal to 0.01 are due to the fact that the PCM appears to have a nearly perfect Lambertian behavior when (part of it) is in solid state [33].

**Table 2.** Input values for the *trans* material used to model the PCM component.

Parameter	Value
Diffuse Reflectance ( $R_{v,diff}$ )	0.32
Diffuse Transmittance ( $T_{v,diff}$ )	0.54
Specular Reflectance ( $R_{v,spec}$ )	0.01
Specular Transmittance ( $T_{v,spec}$ )	0.01

The values used to create the *trans* material in Radiance were suitable to model the PCM in a reliable way. This was based on the spectrophotometrical measures, which showed that both the solid and the liquid state of the PCM are characterized by a fairly constant transmission and reflection coefficient profile throughout the entire visible spectrum, without any particular selective behavior [32,33].

Finally, the selective glass was modelled in Radiance through a *glass* material (featuring a specular transmission), with a visible transmittance  $T_v = 0.5$ .

### 2.3. Performance Metrics and Data Analysis

Two metrics were used to analyze the visual comfort inside the room equipped with the two technologies to be compared: The horizontal illuminance over the workplane and the Daylight Glare Probability (DGP) [10]. The simulation results obtained for the two metrics (each calculated for all the 288 cases) were post-processed through a combined analysis to better describe the visual comfort in the room.

The workplane horizontal illuminance was calculated over a grid of points, positioned 0.75 m above the floor, evenly covering the entire room area (after deducing a peripheral stripe of 50 cm, which is a space typically for the furniture). The grid points (35 in total) were spaced 0.5 m from one another (Figure 1).

In the technical standards [34], the illuminance is one of the metrics used to express the visual comfort in a space. For such a purpose, the average illuminance is coupled with the illuminance uniformity. However, the average workplane illuminance and the illuminance uniformity are not

spatial metrics, i.e., they do not describe the spatial distribution of illuminances over the workplane. For this reason, a new spatial metric was specifically introduced for the purpose of this study: It was named “*Spatial Useful Illuminance*” ( $sE_u$ ) and was defined as the percentage of the grid points whose illuminance lies in the optimal range 100–3000 lx. The lower and upper illuminance ( $E$ ) threshold values were set to 100 lx and 3000 lx, respectively, in accordance with the limits that were introduced by Nabil and Mardaljevic [35] for the Useful Daylight Illuminance ( $UDI$ ). Following the definition by Nabil and Mardaljevic, the  $UDI$  is either: (i) ‘fell-short’, when  $E$  values are insufficient and the occupants turn the electric lights on; (ii) ‘achieved’, when  $E$  values are ‘useful’, that is to say an optimal condition to carry out the visual task without any discomfort; (iii) ‘exceeded’, when  $E$  values may be too high, thus representing a condition that might cause glare for the occupants.

Consistently with this approach, the *Spatial Useful Illuminance* ( $sE_u$ ) adopted in this paper was also structured into three different sub-indexes:  $sE_{u\_100}$  (percentage of workplane with  $E < 100$  lx),  $sE_{u\_100-3000}$  (percentage of workplane with  $E$  in the range 100–3000 lx),  $sE_{u\_3000}$  (percentage of workplane with  $E > 3000$  lx). Although the  $sE_u$  and the  $UDI$  have a similar logic, a conceptual difference needs to be highlighted. While the  $UDI$  gives a *temporal* information, i.e., how frequently throughout a year the illuminance in a point is in a given range, the  $sE_u$  gives a *spatial* information, that is how many points of a grid are in a given illuminance range for a specific time-step. As a comfort goal to pursue, a design should maximize  $sE_{u\_100-3000}$ , while minimizing  $sE_{u\_100}$  and  $sE_{u\_3000}$ , similarly to what should happen with the  $UDI$  (maximize  $UDI_{100-3000}$  while minimizing  $UDI_{100}$  and  $UDI_{3000}$ ).

For glare analyses, the  $DGP$  was calculated for two different points in the room, positioned 1.5 m and 3 m away from the window, at a height of 1.2 m above the floor, to represent a person seated. The view direction was assumed to be perpendicular to the window surface. This is a rather unrealistic condition, as the desks are typically positioned to allow a view direction parallel to the window, but it represents the worst-case scenario in terms of potential glare.

Together with the definition of  $DGP$ , Wienold [36] also provided the reference values to identify a sensation of discomfort for the occupants:

- $DGP < 35\%$ : ‘imperceptible glare’
- $DGP$  in the range 35–40%: ‘perceptible glare’
- $DGP$  in the range 40–45%: ‘disturbing glare’
- $DGP > 45\%$ : ‘intolerable glare’.

A large database of  $sE_u$  and  $DGP$  values ( $DGP_{1.5m}$  and  $DGP_{3m}$ ) was obtained from the simulation of the 288 cases. In detail, for each case, 12 sets of values were found for each metric for the 12 time-steps selected for the analyses. The next step in the study was therefore a synthesis of the results in metrics that allow the “overall” performance of the two technologies to be described, where “overall” refers to the course of a year. For this reason, a temporal average performance throughout the 12 reference time-steps along the year was calculated for each metric, according to the following specifications:

- an average Spatial Useful Illuminance ( $sE_{u,av\_100-3000}$ ), defined as the mean value of all the  $sE_{u\_100-3000}$  values calculated for each of the 12 time-steps. It expresses the percentage of workplane points for which the illuminance is between 100 lx and 3000 lx over the 12 time-steps considered
- two average  $DGP$  ( $DGP_{av}$ ), defined as the mean value of the  $DGP$  values calculated for each of the 12 time-steps, one metric calculated for each of the two points considered in the room for the  $DGP$  calculation ( $DGP_{av\_1.5m}$  and  $DGP_{av\_3m}$ ). Both metrics express the probability of having daylight-related glare issues over the 12 time-steps analyzed.

The number of data to manage was therefore reduced to 12, related to the following remaining variables: The three sites, the two orientations and the two technologies analyzed.

As a further step, the temporal average  $DGP_{av}$  and  $sE_{u,av}$  values were coupled with another analysis. The variation ranges of both the  $sE_{u,av\_100-3000}$  and the  $DGP_{av}$  were subdivided into synthetic



classes. For the  $DGP_{av}$ , the upper and lower thresholds for each class were defined in accordance with the limits set by Reference [36] (Table 3).

**Table 3.** Upper and lower thresholds for each  $DGP_{av}$  class.

Class	Glare Condition	Thresholds
Class A	imperceptible glare	$DGP_{av} < 35\%$
Class B	perceptible glare	$35\% \leq DGP_{av} < 40\%$
Class C	disturbing glare	$40\% \leq DGP_{av} < 45\%$
Class D	intolerable glare	$DGP_{av} \geq 45\%$

For the  $sE_{u,av\_100-3000}$ , no reference has been standardized yet in terms of acceptable and unacceptable ranges. Table 4 summarizes the classification adopted in the present study, so as to have the same number of classes as for the  $DGP$  metric.

**Table 4.** Upper and lower thresholds for each  $sE_{u,av\_100-3000}$  class.

Class	Thresholds
Class A	$sE_{u,av\_100-3000} > 75\%$
Class B	$50\% < sE_{u,av\_100-3000} \leq 75\%$
Class C	$25\% < sE_{u,av\_100-3000} \leq 50\%$
Class D	$sE_{u,av\_100-3000} \leq 25\%$

To some extent, a similar classification can be found in a study from Berardi et al. [37] for the  $UDI_{100-2000}$  metric (percent of occupied time throughout a year when  $E$  values lie in the range 100–2000 lx). In this study, Berardi et al. introduced different classes of performance to describe the daylighting in an office room: “good daylighting” for  $UDI_{100-2000}$  values over 50% (this class further subdivided into two further classes:  $UDI_{100-2000}$  over 75% and  $UDI_{100-2000}$  in the range 50–75%) and “poor daylighting” for  $UDI_{100-2000}$  below 50% (this class further subdivided into two classes:  $UDI_{100-2000}$  between 0% and 25% and  $UDI_{100-2000}$  in the range 25–50%).

The classes A through D were introduced in the present study to express the visual comfort performance of a technology in a synthetic way. The class A actually shows the optimal performance as far as glare control and the Spatial Useful Illuminance  $sE_{u\_100-3000}$  are concerned, while the class D corresponds to the worst performance.

At the end of the post-process phase, the two technologies under investigation were rated (as an average) in two ways: (i) through the 12 time-steps analyzed, in terms of both  $sE_{u\_100-3000}$  and  $DGP$ ; (ii) in terms of occurrence of each class, i.e., how frequent each class is in each of the 12 time-steps. Figure 2 shows an example of the graphical representation that was developed for the purpose of synthetizing the results in just one illustration.

The  $sE_{u,av\_100-3000}$ ,  $DGP_{av\_1.5m}$  and  $DGP_{av\_3m}$  are represented as vertical bars, while the  $sE_u$  and  $DGP$  classes are represented as radial bars. All metrics are expressed in [%], and the reference scale is plotted along the vertical axis to the left of the image. The data for the two technologies are then plotted as mirrored along the horizontal axis, where the PCM glazing data take the upper section and the reference glazing data ( $Sel-0.5$ ) are shown in the lower section of the graph. This graphical representation allows an immediate reading of the results to be obtained and a comparison of the two technologies to be done at a glance. Such representation is meant to be the most viable trade-off to represent a large amount of data in a single chart.

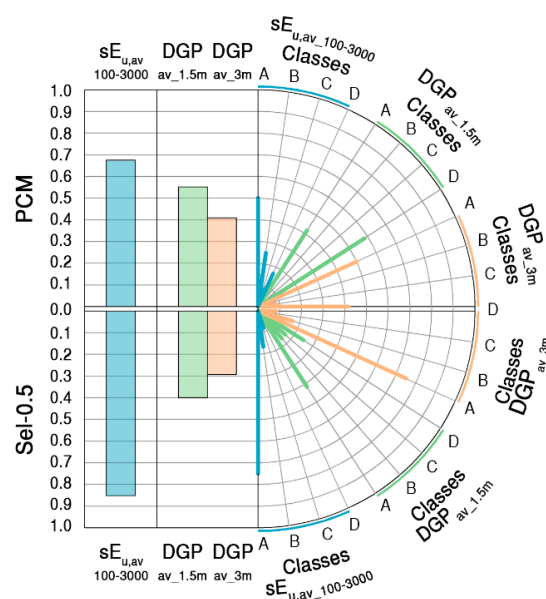


**Figure 2.** Example of synthetic representation of  $sE_{u,av}$  and  $DGP_{av}$  in terms of average values and of classes.

### 3. Results

#### 3.1. Detailed Results of the 288 Cases

The entire set of results from the Radiance simulations are illustrated in Figures 3 and 4, for an overcast sky condition and for a clear sky with sun, respectively.

##### 3.1.1. Overcast Sky Conditions

As expected, the outcomes for the overcast sky condition appear to vary according to the time of the day, the moment of the year and to the geographical site, but not according to the room orientation. In fact, for each location and time-step, the same results were observed for the south and the west orientation. This is due to the inherent characteristics of the CIE Overcast sky model, whose luminance distribution is azimuth-independent. Furthermore, it is worth noting that for every case analyzed,  $sE_{u,3000}$  is always equal to zero: This means that problems of excessive, potentially disturbing light levels on the workplane never occur. On the contrary,  $sE_{u,100}$  (too scarce light level) appears to increase when the sky has low luminance levels, which can happen either early in the morning, at 9.00, or, more frequently, late in the afternoon, at 18:00 or even at 15:00 in the case of Östersund. All the other cases show high values of  $sE_{u,100-3000}$ , mostly up to 100%, which means that the most suitable illuminance conditions are achieved on the workplane to complete the visual task.

The comparison between the PCM and selective glass performance shows an almost equivalent behavior for nearly all the cases analyzed. Some differences occur for low illuminance levels: In these cases, the PCM presents a better performance than the selective glass. As far as the  $DGP$  results are concerned, it is possible to notice that the trends highlighted for  $sE_u$  metric are confirmed, to a great extent. In fact, parallel to a  $sE_{u,3000}$  that is always zero, the  $DGP$  too is always below the value of 35% (imperceptible glare). As expected,  $DGP_{1.5m}$  is always higher than  $DGP_{3m}$ , as it was calculated for a point located closer to the window. The difference between the two  $DGP$  values increases as the sky luminance decreases, since the  $DGP_{3m}$  calculation point is reached by a very low quantity of light. For the cases with a high  $sE_{u,100}$ , the two  $DGP$  values show to be both very low. Although these results were all expected from a theoretical viewpoint, it is possible to draw the conclusion that the PCM glazing shows a better performance than that of the selective glass when the sky luminance is low, under overcast sky conditions.

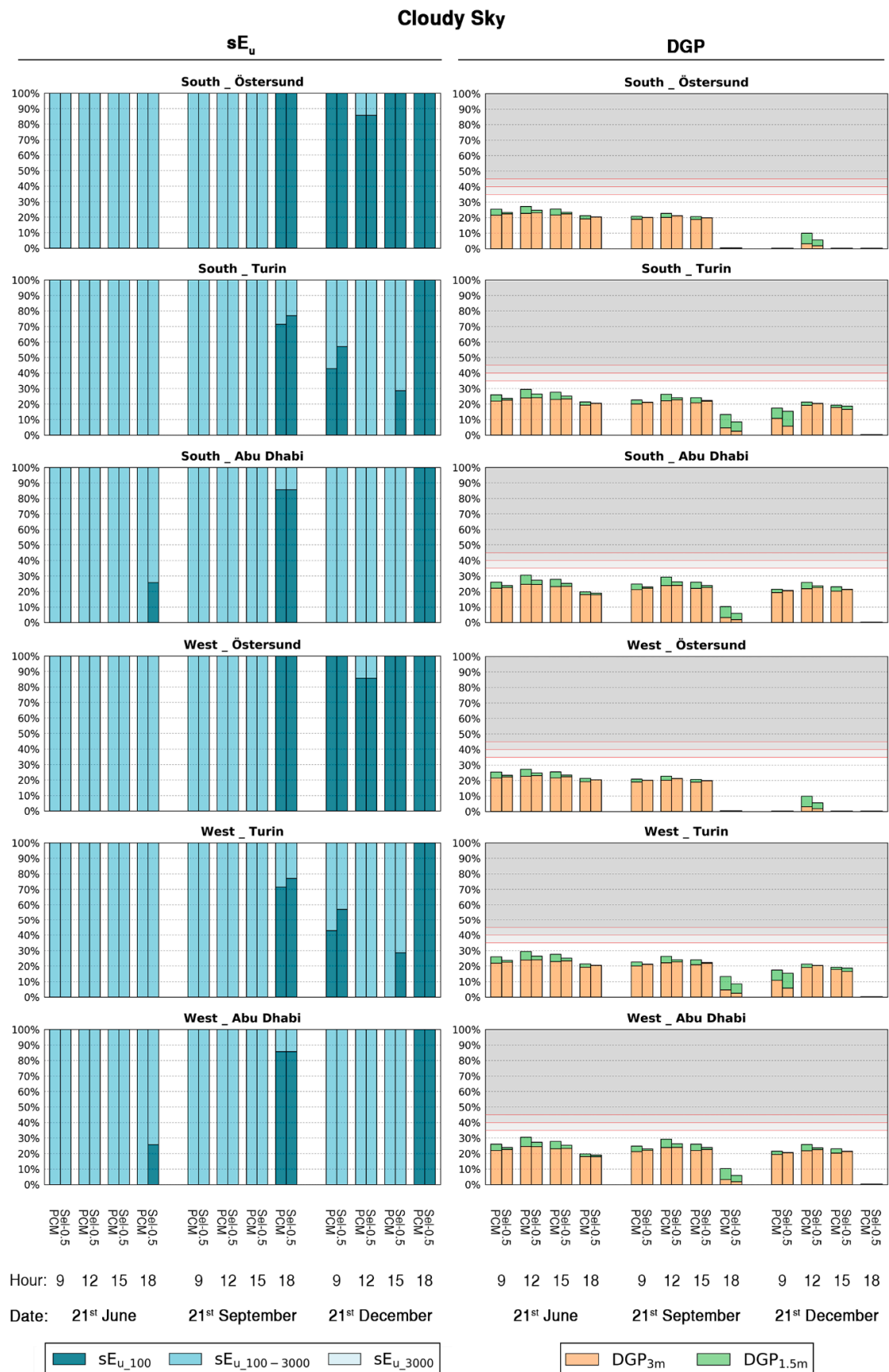
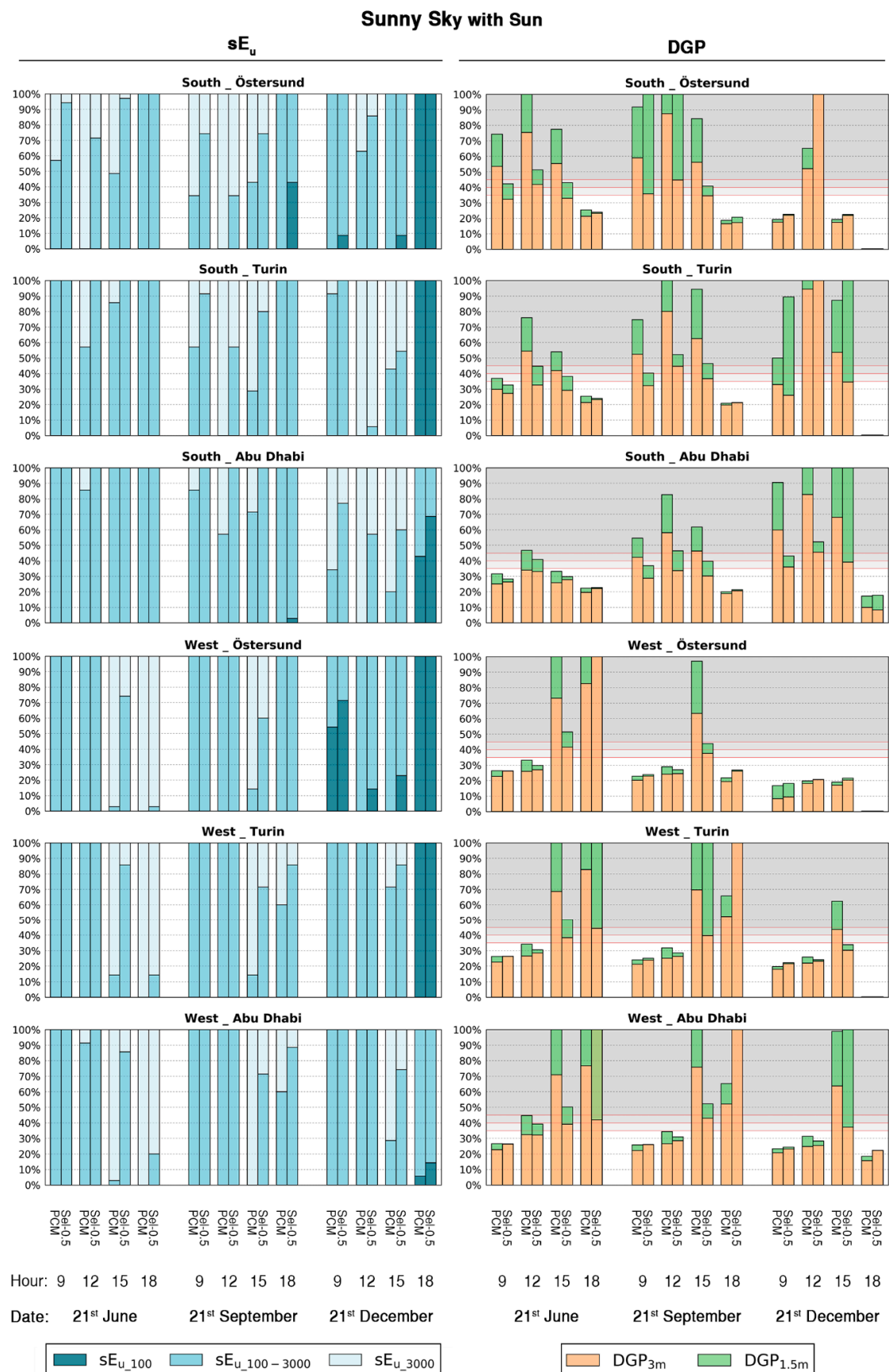


Figure 3.  $sE_u$  and  $DGP$  values obtained for all the cases: overcast sky.



**Figure 4.**  $sE_u$  and DGP values obtained for all the cases: clear sky with sun.

### 3.1.2. Sunny Sky Conditions

Data summarized in Figure 4 show that the performances of the two technologies, when under a sunny sky, differ depending also on the orientation. This means that two cases with similar solar elevation angles but different solar azimuth can have different outcomes. For all the cases, the PCM glazing presents higher  $sE_{u,3000}$  values than the selective glazing. As far as the  $sE_{u,100}$  is concerned, it is possible to observe the same trend that emerged for the overcast sky.  $sE_{u,100}$  raises to high values only for low sun positions in the sky (or after the sunset), and under these conditions, all the cases with the PCM glazing have lower  $sE_{u,100}$  values than the correspondent rooms with the selective glass.

When it comes to the south orientation, it is possible to observe that the  $sE_{u,3000}$  values are always higher for the cases with PCM glazing than for the cases with selective glazing, regardless of the latitude, for the following time: 9:00, 12:00, and 15:00. The  $sE_{u,3000}$  values show a strong dependency on the solar paths specific for the considered site: The difference between the  $sE_{u,3000}$  values for the PCM glazing and for the selective glazing varies in a quite large range (from less than 10% to more than 70%), as a function of the time-step considered (day of the year, hour of the day). The highest  $sE_{u,100-3000}$  values are observed for the summer solstice in Turin and Abu Dhabi, for the autumn equinox in Abu Dhabi, and for the winter solstice in Östersund.

Consistently with their definition, the  $sE_{u,3000}$  and  $sE_{u,100-3000}$  metrics show an opposite trend:  $sE_{u,3000}$  values are generally higher for cases with PCM glazing compared to cases with the conventional selective glazing, while the opposite behavior is observed for  $sE_{u,100-3000}$  values. These trends clearly show that for the same boundary conditions, the DGU with PCM admits more daylighting into the room compared to the DGU with selective glazing, resulting in higher  $sE_{u,3000}$  and in lower  $sE_{u,100-3000}$ . This seems to suggest that the presence of the PCM layer may result in a potential increase in discomfort problems.

The potential glare problems are confirmed by the analysis of  $DGP$  values: For almost all the conditions analyzed, higher  $DGP$  values are observed for cases with the PCM. For most of the cases with a  $sE_{u,3000}$  different than zero, both the  $DGP_{1.5m}$  and  $DGP_{3m}$  are over 45%. The  $DGP_{1.5m}$  values are much lower for the cases with the selective glazing than for those with the PCM, but always over 45%, while for the  $DGP_{3m}$  it is possible to observe less discomfort risk in the presence of the selective glazing ( $DGP < 45\%$ ). The lowest values for  $DGP_{1.5m}$  and  $DGP_{3m}$  are observed for the summer solstice in Abu Dhabi and for the winter solstice in Östersund. For all the other cases, the  $DGP$  for the PCM is classified as intolerable for at least two out of four times of the day.

As far as the west orientation is concerned, an improvement of the  $sE_u$  values is observed for both the technologies under consideration. This is due to reduced issues of excessive, potentially glaring illuminance levels on the workplane at both 9:00 and 12:00. Compared to the south orientation,  $sE_{u,3000}$  is equal to zero in the morning and at noon for all the three sites, except at 12:00 in Abu Dhabi. In the afternoon, when the sun appears in the view through the west-facing window,  $sE_{u,3000}$  values greater than zero occur for all the time-steps until the sunset, with the exception of 21 September at 18:00 in Östersund, when the sun elevation angle is close to  $0^\circ$ . The  $sE_{u,100}$  is greater than zero when the sun has already set ( $sE_{u,100}$  close to 100%) or has a low position over the horizon (in this case,  $sE_{u,100}$  values are lower than the corresponding ones for south-facing rooms).

In a comparative perspective, the PCM glazing leads to higher  $sE_{u,3000}$  values, in the range from less than 10% to more than 80%. The opposite trend applies to the  $sE_{u,100}$  values, which are lower in the presence of the PCM layer. The trend highlighted for the  $sE_u$  is also confirmed for the  $DGP$ : The morning and noon hours show  $DGP$  values always lower than 35% (with one exception only: Abu Dhabi at noon), whilst  $DGP > 45\%$  (intolerable glare) is observed in the afternoon (excluding all cases with low sun position in the sky or after the sunset). Generally speaking, cases with the PCM glazing show higher  $DGP$  values than cases with selective glazing (with the  $DGP_{1.5m}$  generally higher than  $DGP_{3m}$ ), following what already observed for the south orientation.

As previously highlighted, the higher  $sE_{u,3000}$  values and lower  $sE_{u,100}$  values observed for the PCM glazing are a consequence of the fact that the PCM layer globally admits more daylight onto the



workplane. This is due to two factors: (i) the PCM has a higher reflectance property and (ii) there is a directional effect to take into account. If on the one hand it is true that the  $T_v$  of the two glazing systems is similar, on the other hand it is also true that the selective glazing has a specular transmission while the PCM has a Lambertian scattering. This means that when the incidence angle of sunlight hitting the window increases, only a small part of the internal room is hit by the direct sunlight through the selective glazing. When the PCM technology is used, the incident light is scattered inside the ambient along all the directions, and those areas of the room that have low illuminance levels in the presence of the selective glazing receive more daylight with the PCM glazing. This phenomenon also explains the difference between the  $sE_{u,3000}$  calculated for the PCM glazing and for the selective glazing (from less than 10% to more than 80%): This difference is actually smaller for the cases with lower solar incidence angles. When this angle increases, the difference between the  $sE_{u,3000}$  values for the two technologies increase accordingly until when the angle of incidence of the direct radiation reaches a value for which the transmitted radiation becomes far less intense. For solar incidence angles above about  $60^\circ$ , the behavior of the PCM glazing and of the selective glazing becomes similar.

The analyses where the  $DGP$  values are lower for the PCM glazing than for the selective glazing can be explained by considering the different light transmission properties of the two technologies (scattered/diffused versus specular, respectively). When the direct solar radiation hits the  $DGP$  calculation point, the  $DGP$  value for the selective glazing is 100%, while it becomes much lower for the PCM glazing due to its diffusing transmission (however, it never drops below the threshold of 45%, thus remaining in the intolerable range).

Finally, a robust consistency between the  $sE_{u,3000}$  and  $DGP$  metrics is revealed: In most of the cases with  $sE_{u,3000}$  greater than zero a high risk of glare is recorded too, as shown by the  $DGP$  values. This seems to be in line with the latest results of the work by Mardaljevic et al. [38], which led to the upper threshold of the  $UDI$  'exceeded' being increased from 2000 lx to 3000 lx.

### 3.2. Synthetics Representation of Results into Classes

#### 3.2.1. Overcast Sky Conditions

As previously reported in Section 3.1, the outcomes relative to the overcast sky condition show very little variation between the different sites and orientations. For this reason, it was decided not to go through a synthetic representation of these results, as it would show the same class values for almost all the sites and orientations considered.

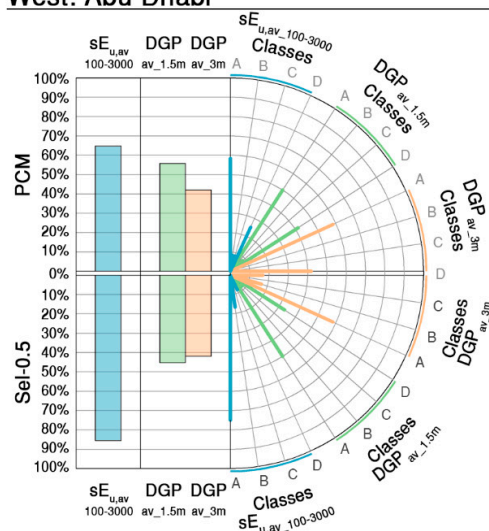
#### 3.2.2. Sunny Sky Conditions

Figure 5 shows the  $sE_u$  and  $DGP$  results, both averaged for the different time-steps analyzed and expressed in classes.

As shown in the figure, the  $sE_{u,av,100-3000}$  values are always higher for the cases with the selective glazing; furthermore, these values are very similar for the two orientations for this technology. Conversely, for the PCM glazing  $sE_{u,av,100-3000}$  values are lower for the south-facing rooms compared to the cases with the selective glazing (constantly around 18%). For the west orientation, this difference ranges from 5% to 20% and increases as the latitude of the site decreases.

With regard to the occurrence of  $sE_u$  classes, for every site, the cases with the selective glazing show a higher occurrence of classes A and B than for the same cases with the PCM glazing, whilst the occurrence of classes C and D is lower. This trend is particularly evident for west-facing rooms: Both the  $DGP_{av,1.5m}$  and the  $DGP_{av,3m}$  values are always higher for cases with the PCM glazing, for all the sites considered. This is consistent with the trends found for the  $sE_{u,av,100-3000}$ . The  $DGP_{av,1.5m}$  and the  $DGP_{av,3m}$  exceed 45% and 35%, respectively, for all the cases considered but for the west-facing rooms in Östersund, where the  $DGP_{av,1.5m}$  value is 40% and the  $DGP_{av,3m}$  value is 31%.





**Figure 5.**  $sE_{u,av\_100-3000}$ ,  $DGP_{av\_1.5m}$ ,  $DGP_{av\_3m}$ ,  $sE_{u,av\_100-3000}$  classes,  $DGP_{av\_1.5m}$  classes and  $DGP_{av\_3m}$  classes. Results for clear sky with sun condition.

The difference of the  $DGP_{av}$  values between the PCM glazing and the selective glazing ranges from 8% to 16% and from 6% to 12%, for  $DGP_{av\_1.5m}$  and for  $DGP_{av\_3m}$  (south orientation), respectively. The difference increases as the latitude decreases for both the  $DGP_{av\_1.5m}$  and the  $DGP_{av\_3m}$ , similarly to what observed for the  $sE_{u,av}$ . For west-facing rooms, the difference is in the range 5–20% for the  $DGP_{av\_1.5m}$  and less than 4% (i.e., negligible) for the  $DGP_{av\_3m}$ . However, no correlation can be established between these values and the latitude of the site. The analysis of the occurrence of the classes for  $DGP_{av\_1.5m}$  and  $DGP_{av\_3m}$  always reveals a better performance of the selective glazing, regardless of the site. For west-facing rooms, occurrence of classes A is equal for the two technologies, but class D values are always sensibly lower for the selective glazing. This finding is in line with what was observed for the metric  $sE_{u,av\_100-3000}$ .

#### 4. Discussion

The originality of this study lies in addressing the evaluation of the performance of a DGU with a PCM layer in terms of the visual comfort perceived by the occupants of a space. The procedure employed to analyze and convey the data is innovative too, and if from the one hand it has been specifically developed for this study, on the other hand it can be adopted for a more general application. A new metric, the “Spatial Useful Illuminance”  $sE_u$  was introduced and coupled to the existing, validated metric  $DGP$  to obtain a comprehensive description of the visual comfort performance of the glazing technologies under consideration. The  $sE_u$  is defined as the fraction of points over the workplane which show an illuminance value in the comfort range 100–3000 lx, while the  $DGP$  quantifies the probability that the occupants perceive glare, and it is based on the vertical illuminance at the eye level. Therefore, the analysis method assesses the visual comfort for the occupants of a space through a combination of two metrics, based on the workplane illuminance and on the eye-level illuminance on a vertical plane.

The  $sE_u$  was defined in accordance with the existing metric  $UDI$ , but while the new metric conveys a spatial information, the established  $UDI$  conveys a temporal information. For both metrics, the illuminance range 100–3000 lx is identified as the optimal lighting condition for the occupants. The  $sE_u$  was then further processed, and through an averaging process and classification in different ranges, the visual comfort performance of the different technologies was expressed in terms of four “performance classes”—A, B, C, D, where class A indicates an optimal performance ( $sE_{u,av}$  in the range 75–100%), while a class D indicates a poor performance ( $sE_{u,av}$  in the range 0–25%).

These performance classes allow a synthetic assessment of the visual comfort performance of any transparent components to be done. For the purpose of this study, the method was applied to evaluate the performance of a DGU with PCM against the performance of a DGU with a selective glazing (with comparable visible transmittance). However, the entire method was conceived so that it can be replicated and applied to other glazing technologies.

Beside the highlighted potentials of this method and the findings of the study, it is also necessary to point out some limitations of the investigation hereby reported. First, all the analyses were carried out assuming that the PCM layer is constantly in solid phase, which means that the liquid and the transient phases were not taken into account. As a result, the PCM was considered as diffusing also for those time-steps (such as, late afternoon hours) when the real material would potentially be in a liquid state. As for the transient phase, this would also perform a diffusing transmission, similar to what has been assumed for the solid phase.

For more accurate analyses, the actual transformation profile of a PCM layer with the different transmission modes should be done, based on the experimental measurement of a bidirectional scattering distribution function. This could be the input for annual simulations where for each time-step the actual transmission property of the PCM is used. Such an approach would allow more reliable results to be obtained, but would be far more time-consuming, not to mention the difficulty in coupling different simulation environments—at present, there is no commercially available energy performance software capable of replicating the thermophysical (and the optical) behavior of PCM

glazing systems, but only on-purpose developed codes are available in the literature (e.g., [21,39,40]); this limitation would require the use of co-simulation to achieve the goal of combining detailed thermal simulations and lighting simulations.

With the simplification adopted in this study, i.e., the PCM constantly in solid phase with a Lambertian diffuse transmission, the PCM glazing was modelled in Radiance in a quite simple way, using a *trans* material. This allowed quicker but still reliable findings to be obtained.

As far as the liquid phase is concerned, previous analyses [32,33] have shown that the light transmission is enhanced, compared to the same glazing without the PCM layer. This (to some extents) “surprising” behavior was explained considering that the refractive index of the PCM layer is very close to that of conventional float glass, and such a feature reduces the optical losses due to the multiple, inter-cavity reflections at the air-glass interface. However, even if this condition of the PCM layer might lead to worse results in terms of visual comfort (too high daylight income), it was decided not to investigate it because of the working conditions of the PCM glazing concept—a well-designed PCM glazing unit should never reach the complete melting state of its PCM layer in order to achieve a good performance, both in terms of energy, thermal comfort, and visual comfort.

The reduced number of time-steps used in the study may be listed as another limitation. Using the two solstices and one equinox (three days), with four hours per each day, was useful to test the novel method and to give the overall assess of the visual comfort performance of the two glazed systems. The different time-steps were chosen to analyze extreme opposite conditions of solar paths during the course of a year, for different latitudes, i.e., to stress the method for a wide range of solar positions. Similarly, the opposite conditions of clear sky (with sun) and overcast sky were tested. However, a more extended analysis of the annual performance of the PCM could be run to obtain more extensive results and more detailed information on an annual basis.

It is worth mentioning that no shading system (neither for the PCM glazing nor for the selective glazing) was simulated in the study. The intent was in fact to evaluate the “pure” performance of the two transparent technologies, which are often used without additional shading devices. However, it is clear that in both cases the addition of a shading system, and the possibility to dynamically control through this device the light transmission (and in the case of the PCM glazing, the interaction between the solar radiation and the PCM) would allow a much better performance to be achieved.

When it comes to the performance classes used in the study, it is important to notice that, for the *DGP*, the classes based on the *DGP* limits defined by Wienold [36] were adopted, while for the  $sE_u$  a set of classes was specifically introduced in this paper. The intervals assumed for the definition of these latter classes are in agreement with the *UDI* classes used by Berardi et al. [37], but they have a different meaning. However, additional investigations might be necessary to assess their robustness and significance.

Finally, it should be observed that the visual comfort was addressed in this study through the  $sE_u$  and the *DGP* metrics only: Other comfort aspects, such as the possibility for the occupants to enjoy a view of the outside, or the possibility of changing the position to avoid the glare were not taken into account. Of course, the assumption of a direction of view perpendicular to the window is not consistent with standard layout of an office, but this choice was in line with the intent of studying the worst-case scenario in terms of risk of glare.

Talking about the possibility of a view to the outside, it is worth pointing out that the presence of a PCM layer in the solid, diffusing state limits the view out. As a result, an optimized layout of the window could imply that the PCM glazing is adopted for the upper and lower sections of the full-height window, leaving a specular (selective) glazing in the middle section as a “view-through” glazing.

## 5. Conclusions

In this paper, the effects produced by a DGU with a PCM layer on the visual environment and the perceived visual comfort for the occupants of a space are presented. A standard DGU with a PCM layer (paraffin wax filling the inter-pane cavity) was simulated and its performance, in terms

of daylighting, compared to that of a conventional DGU with a selective glazing, with similar (total) visible transmittance. The visual comfort inside a sample office space was assessed in terms of *DGP* values (in two points with a different distance from the window) and of “*Spatial Useful Illuminance*”  $sE_u$ , that is the percentage of workplane that shows an illuminance in the comfort range 100–3000 lx.

Due to its light transmission properties, the DGU with the PCM layer generally allows more daylight to be admitted into the space, compared to the DGU with selective glazing. However, the increased amount of daylight compared to the reference case, observed for all the geographical sites, orientations and time-steps considered, does not result, for most cases, in increased visual comfort (evaluated in terms of both  $sE_u$  and of glare risk). On the contrary, a higher daylighting (as shown by higher  $sE_u$  values) corresponds in these cases to an increased glare risk (as shown by increased *DGP* values).

The PCM glazed system shows lower *DGP* values compared to the selective glazed unit when the overall luminance of the portion of sky visible from the window is low. This condition typically occurs in the presence of an overcast sky, or for sunny skies with the sun in lower positions in the sky, or when the sun is not directly visible from the window. Both illuminance levels (assessed in term of  $sE_u$ ) and glare discomfort risk (assessed in term of *DGP*) are lower with the PCM glazing than with the selective glazed unit, for all the sites and orientations analyzed.

Globally, the best performance of the DGU with the PCM layer was observed for the northern location of Östersund: This finding is in accordance with the phenomena observed in the case of low sun elevation angles. However, even in this case, the assessed visual comfort performance of the PCM glazing was worse than that of the selective glazing. In a west-facing room equipped with the PCM glazed unit, the visual comfort performance was found to be slightly better than that of the correspondent south-facing room. This result can again be explained considering the sun’s height over the horizon when it hits west-oriented rooms.

The application of a DGU with a PCM layer, for a façade layout such as the one considered, was shown not to be very favorable in terms of visual comfort provided to the occupants. This is true, to different extents, for all the orientations (south, west) and climates (Östersund, Turin, Abu Dhabi) considered. As already mentioned, a well-designed PCM glazing should be in its transient phase for most of the time (diffusing). Therefore, to provide a view to the outside to the occupants, enhancing thus the visual comfort perceived, such a component should be applied only to part of the façade (for example only to the lower and upper sections of the layout considered). As a result, the negative effects of the PCM glazing on the visual comfort would be significantly reduced, while still preserving part of its benefits on the energy performance. For this reason, architectural applications of a DGU with a PCM layer should be conceived as a trade-off between visual comfort, in terms of daylight availability, glare risk and view to the outside, and energy performance of the space considered.

**Author Contributions:** Conceptualization, F.G. and V.S.; Data curation, L.G.; Formal analysis, L.G. and V.R.M.L.V.; Investigation, L.G.; Methodology, L.G. and V.R.M.L.V.; Supervision, F.G. and V.S.; Writing—original draft, L.G., F.G. and V.R.M.L.V.; Writing—review & editing, F.G., V.R.M.L.V. and V.S.

**Funding:** This research received no external funding.

**Conflicts of Interest:** The authors declare no conflict of interest.

## Acronyms and Symbols

Acronyms	Definition
CIE	Commission Internationale de l’Éclairage
DGU	Double Glazing Unit
PCM	Phase Change Material

Symbols	Definition	Unit
-aa	Ambient accuracy	
-ab	Ambient bounces	
-ad	Ambient divisions	
-ar	Ambient resolution	
-as	Ambient super-samples	
$A_v$	Visible absorptance	[-]
DGP	Daylight Glare Probability	[%]
$DGP_{1.5m}$	Daylight Glare Probability assessed 1.5 m far from the window	[%]
$DGP_{3m}$	Daylight Glare Probability assessed 3 m far from the window	[%]
$DGP_{av}$	Average Daylight Glare Probability	[%]
$DGP_{av_{1.5m}}$	Average Daylight Glare Probability assessed 1.5 m far from the window	[%]
$DGP_{av_{3m}}$	Average Daylight Glare Probability assessed 3 m far from the window	[%]
$E$	Illuminance	[lx]
$L$	Latitude	[°]
$l$	Longitude	[°]
$R_v$	Visible reflectance	[-]
$R_{v,diff}$	Diffuse visible reflectance	[-]
$R_{v,spec}$	Specular visible reflectance	[-]
$Sel-0.5$	DGU with selective glazing	
$sE_u$	Spatial Useful Illuminance	[%]
$sE_{u,av}$	Average Spatial Useful Illuminance	[%]
$sE_{u,av_{100-3000}}$	Average Spatial Useful Illuminance: percentage of workplane with $100 \text{ lx} < E < 3000 \text{ lx}$	[%]
$sE_{u_{100}}$	Spatial Useful Illuminance: percentage of workplane with $E < 100 \text{ lx}$	[%]
$sE_{u_{100-3000}}$	Spatial Useful Illuminance: percentage of workplane with $100 \text{ lx} < E < 3000 \text{ lx}$	[%]
$sE_{u_{3000}}$	Spatial Useful illuminance: percentage of workplane with $E > 3000 \text{ lx}$	[%]
$T_v$	Visible transmittance	[-]
$T_{v,diff}$	Diffuse visible transmittance	[-]
$T_{v,spec}$	Specular visible transmittance	[-]
UDI	Useful Daylight Illuminance	[%]
$UDI_{100}$	Useful Daylight Illuminance: percentage of occupied time for which $E < 100 \text{ lx}$	[%]
$UDI_{100-2000}$	Useful Daylight Illuminance: percentage of occupied time for which $100 \text{ lx} < E < 2000 \text{ lx}$	[%]
$UDI_{100-3000}$	Useful Daylight Illuminance: percentage of occupied time for which $100 \text{ lx} < E < 3000 \text{ lx}$	[%]
$UDI_{3000}$	Useful Daylight Illuminance: percentage of occupied time for which $E > 3000 \text{ lx}$	[%]
$\alpha$	Solar azimuth angle	[°]
$\gamma$	Solar elevation angle	[°]

## References

- Loonen, R.C.G.M. Bio-inspired adaptive building skins. In *Biotechnologies and Biomimetics for Civil Engineering*, 1st ed.; Pacheco Torgal, F., Labrincha, J.A., Diamanti, M.V., Yu, C.P., Lee, H.K., Eds.; Springer International Publishing: Cham, Switzerland, 2015; pp. 115–134. ISBN 978-3-319-09286-7.
- Loonen, R.C.G.M.; Trčka, M.; Cóstola, D.; Hensen, J.L.M. Climate adaptive building shells: State-of-the-art and future challenges. *Renew. Sustain. Energy Rev.* **2013**, *25*, 483–493. [\[CrossRef\]](#)
- Baetens, R.; Jelle, B.P.; Gustavsen, A. Properties, requirements and possibilities of smart windows for dynamic daylight and solar energy control in buildings: A state-of-the-art review. *Sol. Energy Mater. Sol. C* **2010**, *94*, 87–105. [\[CrossRef\]](#)
- Jiru, T.E.; Taob, Y.X.; Haghighat, F. Airflow and heat transfer in double skin facades. *Energy Build.* **2011**, *43*, 2760–2766. [\[CrossRef\]](#)
- Shameri, M.A.; Alghoul, M.A.; Sopian, K.; Zain, M.F.M.; Elayeb, O. Perspectives of double skin façade systems in buildings and energy saving. *Renew. Sustain. Energy Rev.* **2011**, *15*, 1468–1475. [\[CrossRef\]](#)
- Silva, T.; Vicente, R.; Rodrigues, F. Literature review on the use of phase change materials in glazing and shading solutions. *Renew. Sustain. Energy Rev.* **2016**, *53*, 515–535. [\[CrossRef\]](#)

7. Andersen, M. Unweaving the human response in daylighting design. *Build. Environ.* **2014**, *91*, 101–117. [[CrossRef](#)]
8. Carlucci, S.; Causone, F.; De Rosa, F.; Pagliano, L. A review of indices for assessing visual comfort with a view to their use in optimization processes to support building integrated design. *Renew. Sustain. Energy Rev.* **2015**, *47*, 1016–1033. [[CrossRef](#)]
9. European Committee for Standardisation. *EN 12665, Light and Lighting—Basic Terms and Criteria for Specifying Lighting Requirements*; European Committee for Standardisation: Brussels, Belgium, 2011.
10. Wienold, J.; Christoffersen, J. Evaluation methods and development of a new glare prediction model for daylight environments with the use of CCD cameras. *Energy Build.* **2006**, *38*, 743–757. [[CrossRef](#)]
11. Konstantzos, I.; Tzempelikos, A.; Chan, Y.C. Experimental and simulation analysis of daylight glare probability in offices with dynamic window shades. *Build. Environ.* **2015**, *87*, 244–254. [[CrossRef](#)]
12. Piccolo, A.; Simone, F. Effect of switchable glazing on discomfort glare from windows. *Build. Environ.* **2009**, *44*, 1171–1180. [[CrossRef](#)]
13. Matusiak, B.S. Glare from a translucent façade, evaluation with an experimental method. *Sol. Energy* **2013**, *97*, 230–237. [[CrossRef](#)]
14. Aries, M.B.C.; Veitch, J.A.; Newsham, G.R. Windows, view, and office characteristics predict physical and psychological discomfort. *J. Environ. Psychol.* **2010**, *30*, 533–541. [[CrossRef](#)]
15. Tuaycharoen, N.; Tregenza, P.R. View and discomfort glare from windows. *Light. Res. Technol.* **2007**, *39*, 185–200. [[CrossRef](#)]
16. Fokaides, P.A.; Kylili, A.; Kalogirou, S.A. Phase change materials (PCMs) integrated into transparent building elements: A review. *Mater. Renew. Sustain. Energy* **2015**, *4*. [[CrossRef](#)]
17. Vigna, I.; Bianco, L.; Goia, F.; Serra, V. Phase Change Materials in Transparent Building Envelopes: A Strengths, Weakness, Opportunities and Threats (SWOT) Analysis. *Energies* **2018**, *11*, 111. [[CrossRef](#)]
18. Giovannini, L.; Goia, F.; Lo Verso, V.R.M.; Serra, V. Phase Change Materials in glazing: implications on light distribution and visual comfort. Preliminary results. *Energy Proc.* **2017**, *111*, 357–366. [[CrossRef](#)]
19. Goia, F.; Perino, M.; Serra, V. Improving thermal comfort conditions by means of PCM glazing systems. *Energy Build.* **2013**, *60*, 442–452. [[CrossRef](#)]
20. Goia, F.; Perino, M.; Serra, V. Experimental analysis of the energy performance of a full-scale PCM glazing prototype. *Sol. Energy* **2014**, *100*, 217–233. [[CrossRef](#)]
21. Gowreesunker, B.L.; Stankovic, S.B.; Tassou, S.A.; Kyriacou, P.A. Experimental and numerical investigations of the optical and thermal aspects of a PCM-glazed unit. *Energy Build.* **2013**, *61*, 239–249. [[CrossRef](#)]
22. Ismail, K.; Henríquez, J. Parametric study on composite and PCM glass systems. *Energy Convers. Manag.* **2002**, *43*, 973–993. [[CrossRef](#)]
23. Li, S.; Zhou, Y.; Zhong, K.; Zhang, X.; Jin, X. Thermal analysis of PCM-filled glass windows in hot summer and cold winter area. *Int. J. Low-Carbon Technol.* **2013**, *11*, 1–8. [[CrossRef](#)]
24. Goia, F. Thermo-physical behaviour and energy performance assessment of PCM glazing system configurations: A numerical analysis. *Front. Arch. Res.* **2012**, *1*, 341–347. [[CrossRef](#)]
25. Weinläder, H.; Beck, A.; Fricke, J. PCM-façade-panel for daylighting and room heating. *Sol. Energy* **2005**, *78*, 177–186. [[CrossRef](#)]
26. Goia, F.; Bianco, L.; Cascone, Y.; Perino, M.; Serra, V. Experimental analysis of an advanced dynamic glazing prototype integrating PCM and thermotropic layers. *Energy Proc.* **2014**, *48*, 1272–1281. [[CrossRef](#)]
27. Iennarella, S.; Lo Verso, V.R.M.; Serra, V. A novel concept of a responsive transparent façade module: optimization of energy performance through parametric design. *Energy Proc.* **2015**, *78*, 358–363. [[CrossRef](#)]
28. Frontini, F.; Pfefferot, J.; Herkel, S.; Schwartz, D. Building simulation study of a residential double-row, house with seasonal PCM-translucent façade. In *Proceedings of the CISBAT 2011-International Conference—CleanTech for Sustainable Buildings—From Nano to Urban Scale*, Lausanne, Switzerland, 11–16 September 2011; pp. 99–104.
29. Grynning, S.; Goia, F.; Time, B. Dynamic Thermal Performance of a PCM Window System: Characterization Using Large Scale Measurements. *Energy Proc.* **2015**, *78*, 85–90. [[CrossRef](#)]
30. Grynning, S.; Goia, F.; Rognvik, E.; Time, B. Possibilities for characterization of a PCM window system using large scale measurements. *Int. J. Sustain. Built. Environ.* **2013**, *2*, 56–64. [[CrossRef](#)]
31. Manz, H.; Egolf, P.W.; Suter, P.; Goetzberger, A.; Abel, E. TIM—PCM external wall system for solar space heating and daylighting. *Sol. Energy* **1997**, *61*, 369–379. [[CrossRef](#)]



32. Goia, F.; Zinzi, M.; Carnielo, E.; Serra, V. Characterization of the optical properties of a PCM glazing system. *Energy Proc.* **2012**, *30*, 428–437. [[CrossRef](#)]
33. Goia, F.; Zinzi, M.; Carnielo, E.; Serra, V. Spectral and angular solar properties of a PCM-filled double glazing unit. *Energy Build.* **2015**, *87*, 302–312. [[CrossRef](#)]
34. European Committee for Standardisation. *EN 12464, Light and Lighting—Lighting of Workplaces Part 1: Indoor Work Places*; European Committee for Standardisation: Brussels, Belgium, 2011.
35. Nabil, A.; Mardaljevic, J. Useful daylight illuminance: a new paradigm for assessing daylight in buildings. *Light. Res. Technol.* **2005**, *37*, 41–59. [[CrossRef](#)]
36. Wienold, J. Dynamic daylight glare evaluation. In Proceedings of the 11th International IBPSA (International Building Performance Simulation Association) Conference—Building Simulation, Glasgow, Scotland, 27–30 July 2009; pp. 944–951.
37. Berardi, U.; Hamid Anaraki, K. Analysis of the Impacts of Light Shelves on the Useful Daylight Illuminance in Office Buildings in Toronto. *Energy Proc.* **2015**, *78*, 1793–1798. [[CrossRef](#)]
38. Mardaljevic, J.; Andersen, M.; Roy, N.; Christoffersen, J. Daylighting metrics for residential buildings. In Proceedings of the 27th Session of CIE, Sun City, South Africa, 11–15 July 2011; pp. 93–111.
39. Goia, F.; Perino, M.; Haase, M. A numerical model to evaluate the thermal behaviour of PCM glazing system configurations. *Energy Build.* **2012**, *54*, 141–153. [[CrossRef](#)]
40. Liu, C.; Zhou, Y.; Li, D.; Meng, F.; Zheng, Y.; Liu, X. Numerical analysis on thermal performance of a PCM-filled double glazing roof. *Energy Build.* **2016**, *125*, 267–275. [[CrossRef](#)]



© 2018 by the authors. Licensee MDPI, Basel, Switzerland. This article is an open access article distributed under the terms and conditions of the Creative Commons Attribution (CC BY) license (<http://creativecommons.org/licenses/by/4.0/>).